3D SCENE RECONSTRUCTION AND PATH PLANNING METHOD FOR UAV IN GNSS-DENIED ENVIRONMENT

Qingeng Jin[1], Pengcheng Zhao[1], Qingwu Hu[1,*], Xuzhe Duan[1], Mingyao Ai[1]

[1] School of Remote Sensing and Information Engineering, Wuhan University, Wuhan 430079, China,
(jin_qg, pengcheng.zhao, huqw, duanxz, aimingyao)@whu.edu.cn

KEY WORDS: GNSS-denied, UAV, Laser SLAM, Path Planning and Optimization, PRM.

ABSTRACT:

Today, natural disasters have a huge impact all over the world, while GNSS plays an important role in disaster relief and rescue. However, when the ground surface is severely damaged and covered, satellite positioning means are denied. In addition, disaster site conditions are often very complex and may require unmanned robots such as UAVs for pre-surveying. To address the raised problem, we reconstructed the 3D scene by laser SLAM; improved PRM path planning method for better computational efficiency while solving feasible path results; and realized UAV autonomous flight along the planned path in GNSS-denied environment. The experiments prove that the reconstructed scene map provides a feasible means for UAV autonomous navigation in GNSS-denied environment, and the proposed path planning method has a significant improvement in computational efficiency.

1. INTRODUCTION

Natural disasters have brought undeniable impacts to all countries and regions of the world, threatening human lives and safety, as well as interfering with economic and social development. Satellites play an important role in the monitoring and assessment of disasters. Satellite remote sensing (Rees, 2013) is available to assist in the monitoring and management of disasters (Kaku, 2019), while Global Navigation Satellite System (GNSS) (Hofmann-Wellenhof et al., 2007) can provide location information for emergency rescue. However, when natural disasters cause serious damage to the ground surface resulting in it being covered and obscured, signals from traditional satellites have difficulty reaching the ground thus cannot obtain the real situation on the ground. This makes satellite remote sensing failed and satellite positioning denied, bringing difficulties and challenges to disaster relief and rescue. Therefore, we need to develop new means of environmental sensing and positioning, and integrate them into emergency equipment such as unmanned aerial vehicles (UAVs), in order to achieve rapid reconstruction and localization of damaged areas.

The 3D scene is reconstructed using UAV to serve as a map for the priori knowledge of path planning. Models of the buildings are widely used, such as Building Information Modeling (BIM) (Xu et al., 2017) and terrain models (Dehbi et al., 2020). However, the buildings are likely to be severely damaged by natural disasters, so that the previous model will not be able to correctly represent the actual situation. There are also methods to reconstruct the scene based on images and perform path planning (Zhang et al., 2020), but optical images require good lighting conditions in the scene, which is difficult to meet after a power outage caused by disasters. In contrast, light detection and ranging (LiDAR) technology works in a poor lighting environment, and rapid 3D scene reconstruction by the UAV with LiDAR has proven to be effective (Chiang et al., 2017).

Based on LiDAR, laser simultaneous localization and mapping (SLAM) (Bailey, Durrant-Whyte, 2006) provides a feasible method for 3D scene mapping and local navigation. Hector SLAM (Kohlbrecher et al., 2011) achieves point cloud matching by aligning point clouds to grid maps. LiDAR odometry and mapping (LOAM) (Zhang, Singh, 2014) splits the task into high-frequency localization and low-frequency mapping, which substantially improves real-time performance. LiDAR inertial odometry via smoothing and mapping (LIO-SAM) (Shan et al., 2020) adds an inertial measurement unit (IMU) pre-integration factor to the SLAM back-end for factor graph optimization. Fast direct LiDAR-inertial odometry (FAST-LIO) (Xu, Zhang, 2021) fuses feature point data of IMU and LiDAR, which can cope with fast motion and noisy environments. Following some recommended strategies (Karam et al., 2020), laser SLAM can well meet both outdoor and indoor mapping requirements. Laser SLAM can achieve autonomous localization without relying on GNSS and is adaptable in environments with poor lighting conditions, which can play a unique role in disaster relief and rescue.

Maps of the disaster scene are the basis for navigation, according to which ambulance crews recognize the situation and carry out rescue. However, when the disaster scene is too complex and unpredictable, it is safer to use unmanned robots for pre-search, especially UAVs with better manoeuvrability. Therefore, it is also critical to plan search paths for UAVs based on disaster scene maps. Considering the complexity and uncertainty of the disaster scene, the path planning algorithm has to ensure its robustness and efficiency. As a result, graph-based path planning algorithms are more suitable for this application because they are often simpler and faster.

The research on graph-based path planning is maturely developed. A* (Hart et al., 1968) and D* (Ferguson, Stentz, 2007) are both commonly used path search algorithms, they are both heuristic search methods to obtain a best path by predicting a minimum cost. Besides, rapidly exploring random tree (RRT) can also be used in UAV path planning (Yin et al.,

* Corresponding author

https://doi.org/10.5194/isprs-annals-X-3-W1-2022-69-2022

2017), which is based on random sampling to continuously expand a tree-like search path from the start. It is fast in exploration but not guaranteed to obtain an optimal path. Probabilistic roadmap (PRM) also has advantages and is applied to the quadrotor UAV (Chen et al., 2019). It constructs a connection network by random sampling in the map and then performs path search on the network, which has the capability of finding a better path.

In this paper, we proposed a 3D scene reconstruction and path planning method for UAV in GNSS-denied environment. The 3D scene is reconstructed by laser SLAM; the PRM path planning method is improved for better computational efficiency while solving feasible path results; and the UAV flight is realized in GNSS-denied environment where the UAV can autonomously fly along the planned path.

2. METHODOLOGY

The workflow of our method is shown in Figure 1, consisting of the following parts:

1. Laser SLAM, to capture the point cloud of the 3D scene frame by frame and estimate the pose of the UAV during scanning.
2. Grid map generation, to produce a basis map for path planning and navigation.
3. Improved PRM path planning, to rationally construct a connection network, adaptively update and search for a collision-free path.
4. Path optimization, to obtain a straightforward and feasible path by reordering waypoints in the path.
5. UAV positioning and navigation control, to implement the autonomous flight along planned path in GNSS-denied environment.

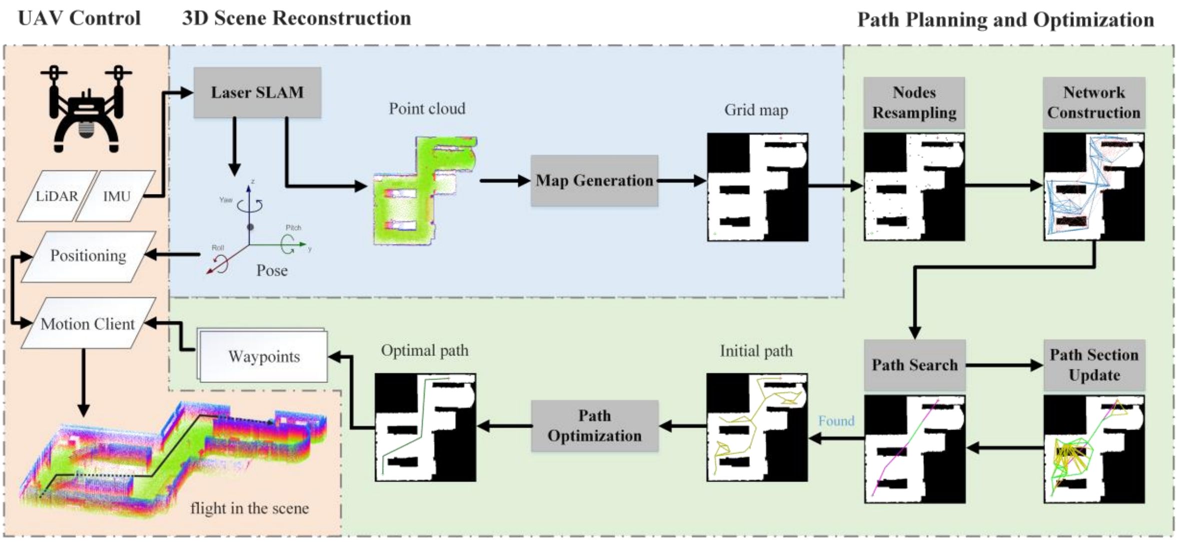

Figure 1. Workflow of our method.

2.1 3D Scene Reconstruction Based on Laser SLAM

Based on laser SLAM, GNSS is not required in our method of 3D scene reconstruction which is efficiently achieved with only two kinds of sensors, LiDAR and IMU. Laser SLAM is divided into two parts: front-end and back-end.

The SLAM front-end is mainly to estimate real-time state of the UAV based on sensor fusion. The commonly used sensor fusion method is Kalman filter (Welch, 2020). The point cloud of the 3D scene is acquired using LiDAR, and the UAV pose is estimated using IMU. They respectively form the observation and prediction equations in the Kalman filter framework. Solving the equation, we can obtain the UAV pose state at every corresponding moment.

The SLAM back-end is mainly to optimize the historical state of the UAV. We use factor graph (Indelman et al., 2012) to constrain the odometry and IMU pre-integration and obtain a maximum posteriori estimation by measuring the residuals, which is essentially defining and solving a least squares problem, i.e., achieving further correction of the UAV historical state by nonlinear optimization. The advantage of the factor graph method is that it transforms the action of various constraints into a product of factors, simplifying the computation while allowing the convenient inclusion of different constraints.

According to the optimized historical state sequence of the UAV, each frame of the point cloud is transformed according to the UAV pose at the moment of its observation, and then all transformed point clouds are fused to a global point cloud. Based on this global point cloud, we can then construct a map of the scene. Firstly, the spatial entities such as ceiling and floor are identified by detecting the plane and segmented out from the global point cloud. Secondly, the initial top view of the 3D scene is constructed based on the remaining point cloud using a projection method. Finally, the scene top view is converted into a binary grid map. The grid map is divided into obstacle grids and free grids. An obstacle grid represents a square area that cannot be occupied or passed, while a free grid represents an area that can be traversed and hovered by the UAV. The grid map is used as the navigation map for path planning.

2.2 Connection Network Initialization

PRM is a graph-based path planning method. It randomly samples in the map as candidate nodes and adds connected edges between those which are visible to each other, thus construct a connection network. To better distinguish the edges,

https://doi.org/10.5194/isprs-annals-X-3-W1-2022-69-2022

we divide them into two categories and simply name the edges that have two visible nodes as good edges, and the other as bad edges. The path search is performed on the connection network to obtain a path from the start to the end.

The most time-consuming part of the basic PRM method is the connectivity check of the nodes, so we adopt some strategies in order to reduce the computational effort and improve the computational efficiency. The improvement strategies include specifying the connection distance and incrementally updating the path sections.

To initialize the connection network, firstly, a certain number of points are randomly sampled in free grids of the map as candidate nodes of the connection network. Secondly, a threshold of connection distance is set, and the connections between nodes smaller than this threshold are regarded as candidate edges, which are checked for connectivity later. The connection networks under different connection distances are shown in Figure 2.

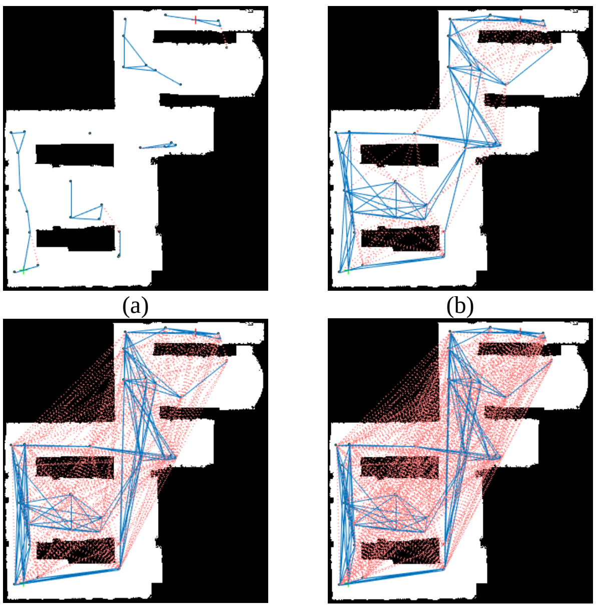

(a) (b) (c) (d)

Figure 2. Connection network under different connection distances of 0.1 (a), 0.25 (b), 0.5 (c) and 1 (d). The blue and red lines represent the good and bad edges.

The connection distance threshold should be adapted to the number of sampling points. When there is a small number of sampling points, the threshold should be increased, otherwise it may lead to a shortage of effective edges in the initial network; when there is a large number of sampling points, the threshold should be reduced, otherwise it may lead to many redundant edges in the initial network, bringing unnecessary checks and a decrease in search efficiency.

2.3 Path Section Incremental Update and Search

We set a threshold of connection distance during the network initialization to reduce ineffective checks, since inter-node connectivity checks requires much computation, and nodes that are farther away are more likely to be blocked by obstacles in the scene, so calculating their connectivity is not effective in increasing the overall connectivity of the network. In addition, as a result of the greedy strategy that the path search adopts, not all edges in the network will be searched. Instead of checking connectivity of all candidate edges after initialization, we directly start path searching and perform connectivity checks during searching, and update the network after each check.

During path searching, only the currently searched edge is checked for connectivity. If the edge collides with obstacle grids in the map, it will be removed from the network, then we search for a new path that can connect the two nodes of the removed edge; if the edge passes the collision check, it will be added to the result path, and then we continue searching backward. These steps are repeated until we obtain a collision-free path from the start to the end, as shown in Figure 3.

The method of incremental update and search greatly reduces the number of collision checks for they are performed only when needed. Not only does this method improve computational efficiency, but the path is collision-free with the obstacles, ensuring a safe flight for UAV in the scene.

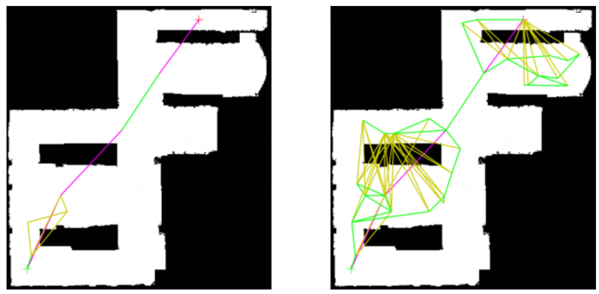

(a) (b)

Figure 3. Path sections before (a) and after (b) update.

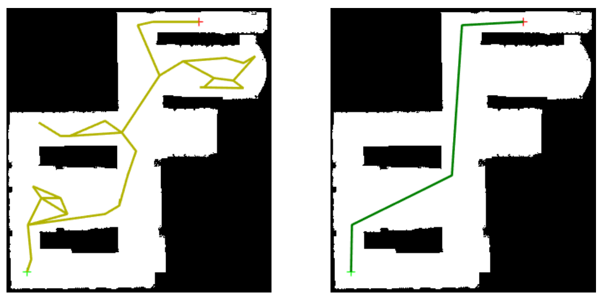

(a) (b)

Figure 4. Path before (a) and after (b) optimization.

2.4 Waypoint Optimization

We name the initially searched path as candidate path which consists of candidate waypoints for the UAV flight. With the incremental update of path sections, on the one hand, we ensure that the candidate path is collision-free with the environment, on the other hand, we cannot ensure that it is straightforward and smooth. This is because the two nodes on each side of a checked edge are always fixed during updating, based on which we search for new connections. Despite the fact that this strategy may lead to unnecessary detours, it is still possible to obtain a shorter and smoother path if we reorder and remove redundant waypoints in the candidate path.

In order to further optimize the candidate path, we perform cross-waypoint connectivity check for each candidate waypoint in the path. If two distant and non-adjacent waypoints are visible to each other, we directly reconnect them and discard the other waypoints in between.

With this waypoint optimization method, we can obtain a straightforward optimal path, as shown in Figure 4. The optimal path helps to achieve better motion of the UAV along the waypoints, reduces energy loss due to severe pose changes as well as improves safety of the flight. As for path smoothness, there is little need to further optimize the path for its smoothness, since the UAV we use is a quadcopter which has few motion constraints, it has very low requirements for the smoothness of the path. However, the result path can easily be further optimized by curve generation methods, e.g., B-splines (Stoican et al., 2017), Bezier curves (Faigl, Váňa, 2018).

2.5 UAV Positioning and Navigation in GNSS-denied Environment

In the “3D Scene Reconstruction Based on Laser SLAM” section, we use laser SLAM to record the real-time pose state of the UAV, which can be used as the reference for positioning in GNSS-denied environment. In addition to the tasks of take-off and landing, the UAV calculates its real-time distance to the waypoint goal and flies toward it during the flight. The UAV will switch to the next waypoint after reaching the current one, until it traverses all the waypoints in the path, thus completes the flight task.

3. EXPERIMENTS

Our path planning and optimization method has been tested in three cases:

1. The first case is an indoor scene of low complexity, as shown in Figure 5(a). It is a hall where the main obstacles are two staircases.
2. The second case is also an indoor scene but it is of higher complexity, as shown in Figure 5(c). It is a whole floor of office area, which is divided into several rooms and corridors.
3. The third case is an outdoor scene, as shown in Figure 5(b). We deliberately left a lot of noise in this case in order to test the robustness of our method.

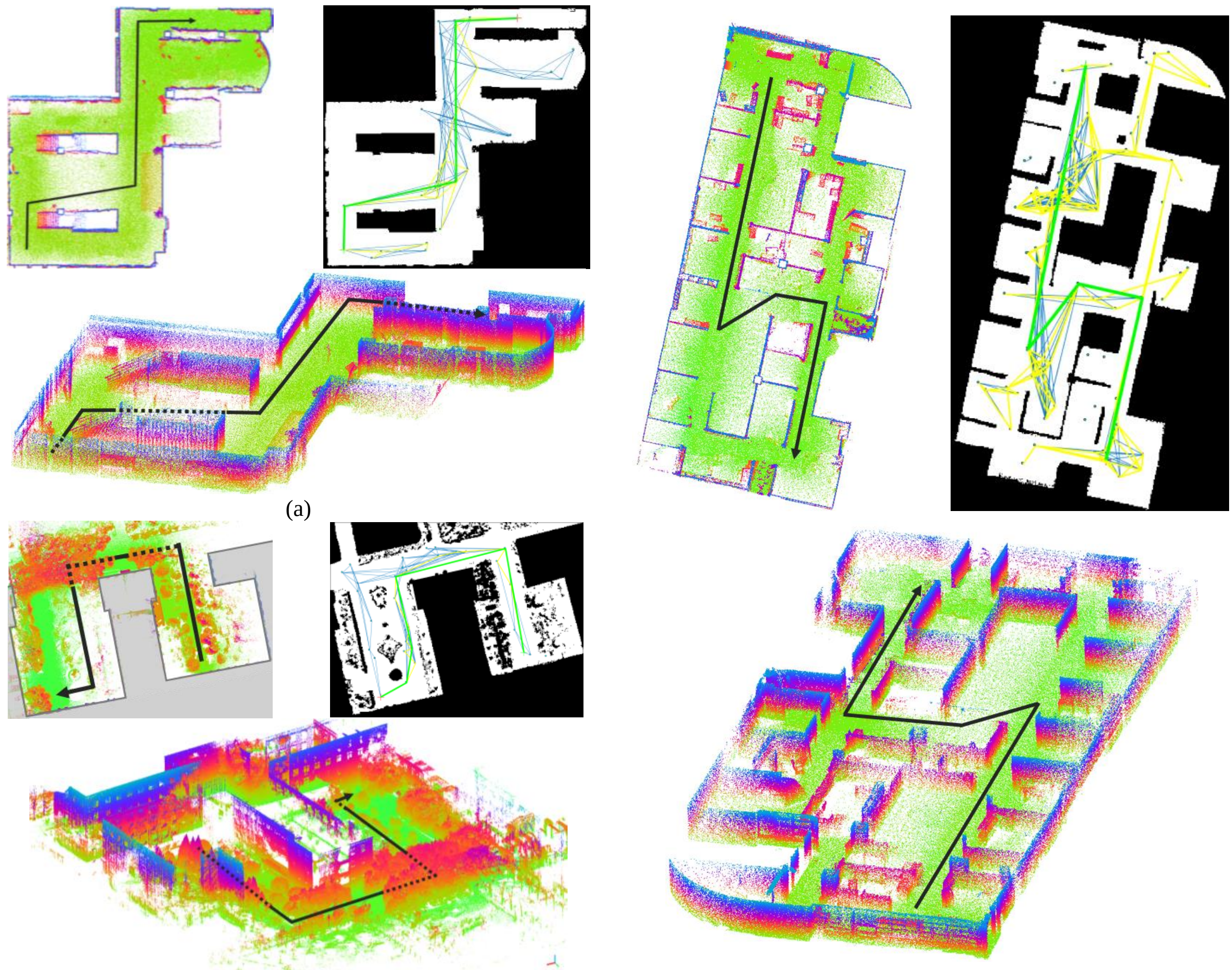

(a) (b) (c)

Figure 5. Point cloud and planning results of Map 1 (a), Map 2(c) and Map 3 (b). The first row of each sub-figure is the top view of its point cloud and planning result, and the second row is the overview of the point cloud from another angle. In the figures of point clouds, the point clouds are rendered in height ramp, and the black lines represents the path result. In the figures of planning results, the blue lines represent the edges in the connection network, the yellow lines represent the updated path sections, the cyan lines represent the collision-free path before optimization, and the green lines represent the finally optimal path.

https://doi.org/10.5194/isprs-annals-X-3-W1-2022-69-2022

It should be noted that there are some blank areas in the original point cloud due to the lack of scans. For the safety reason, we regard them as impassable and treat them as obstacle grids in the map. We performed our planning method after selecting the start and end grids in two farthest rooms which locates in the diagonal direction on the maps. The planning results are shown in Figure 5. For simplicity, we name the grid maps of these scenes as Map 1, Map 2 and Map 3.

We implemented the path planning and optimization method in MATLAB, after processing the point clouds using Point Cloud Library (PCL). The computer configuration is Intel® Core^{TM} i7-6700 3.40GHz CPU with 8GB of RAM. We loaded the LiDAR and IMU sensors on the UAV, as shown in Figure 6, achieving autonomous navigation and flight.

Figure 6. Our UAV with LiDAR and IMU sensors below.

To illustrate the effectiveness and efficiency of our method, we use planning time and path length as evaluation metrics. The planning time is the time for the method to solve a feasible and optimal path from the start to the end in the map, including the time for initializing connection network, updating, searching and optimizing the path. It reflects our improvements in planning efficiency. The path length is the length of the finally optimal path, which reflects the effectiveness of our path optimization method. In addition, due to the randomness of sampling in PRM algorithm, we chose several sets of representative results for analysis. The experimental results are listed in Table 1.

Comparing the planning time under different number of nodes and connection distances, as shown in the first row of Figure 7, we found that the planning time of the basic PRM method is mainly consumed by network initialization, while the time of our method is mainly consumed by path section update and search. The reason why our method is superior to the basic one is that, time consumed by the basic method in network initialization increases linearly as the number of nodes increases, while the redundancy of the network increases at the same time. In our method, on the contrary, connectivity checks are performed only when needed. Therefore, time for network initialization maintains a steady change, and time for update and search is better utilized to expand the path. Although our method needs additional path optimization, it has little impact on the planning time. As a result, our method can critically reduce the planning time in simple scenes and also has advantages in complex scenes. Besides, it also shows computational efficiency in the presence of noise.

Node num.	Connection distance	Edge num.				Time (basic PRM)		Time (ours)		
		Good	Bad	Skipped	Updated	Init.	Search	Init.	Update	Opt.
Map 1										
30	0.25	110	93	293	36	0.854	0.013	0.010	0.283	0.201
	0.5	157	275	64	7	2.123	0.014	0.007	0.144	0.160
	1	159	337	0	8	2.440	0.014	0.008	0.163	0.167
50	0.25	287	254	785	40	2.234	0.016	0.010	0.363	0.220
	0.5	366	743	217	47	5.217	0.018	0.012	0.364	0.218
	1	371	955	0	48	6.292	0.015	0.012	0.392	0.223
70	0.25	552	438	1566	53	4.328	0.021	0.010	0.292	0.281
	0.5	728	1448	380	57	10.540	0.021	0.016	0.321	0.305
	1	749	1807	0	59	12.336	0.024	0.018	0.412	0.308
Map 2										
75	0.25	271	1026	1629	843	3.723	0.016	0.011	4.335	0.311
	0.5	294	2232	400	1430	7.961	0.015	0.023	8.105	0.205
	1	297	2629	0	1497	9.805	0.015	0.019	9.274	0.202
100	0.25	584	1610	2957	702	6.136	0.019	0.024	3.155	0.295
	0.5	613	3472	1066	1454	12.572	0.018	0.027	8.936	0.403
	1	617	4534	0	1456	19.783	0.021	0.034	9.303	0.400
125	0.25	800	2576	4625	1521	10.297	0.018	0.050	7.350	0.301
	0.5	820	5191	1990	3190	19.184	0.020	0.034	20.437	0.292
	1	825	7176	0	3098	25.664	0.019	0.039	20.544	0.196
Map 3										
30	0.25	96	103	297	13	0.770	0.019	0.007	0.109	0.215
	0.5	115	341	40	47	1.624	0.019	0.008	0.242	0.258
	1	116	380	0	71	1.763	0.019	0.007	0.456	0.295
50	0.25	234	223	869	162	1.619	0.019	0.011	0.935	0.424
	0.5	313	866	147	264	4.286	0.017	0.013	1.233	0.310
	1	314	1012	0	264	4.639	0.015	0.015	1.237	0.307
70	0.25	486	497	1573	33	3.341	0.019	0.019	0.162	0.233
	0.5	558	1681	317	108	6.824	0.020	0.017	0.438	0.611
	1	564	1992	0	108	7.451	0.020	0.019	0.435	0.605

Table 1. Experimental results.

https://doi.org/10.5194/isprs-annals-X-3-W1-2022-69-2022

Comparing the path lengths obtained under the same number of nodes and different connection distances, as shown in the second row of Figure 7, we found that the candidate path is often not optimal due to the shortage of network edges when the connection distance is small, but our method has a good effect on shortening its length. With the connection distance increasing, the path length of our method gradually approaches the path length of the basic PRM. Although our path length may be slightly larger than that of the basic PRM, which is because we use an incremental search strategy instead of a global one, it is still well worth the sacrifice for computational efficiency, especially in an unpredictable and dangerous situation after a disaster, where we solve a path the sooner the better.

In summary, our path planning method greatly improves the computational efficiency compared to the basic PRM method, while keeping reasonable length of the result path with optimization. Moreover, it also shows a good performance in the presence of noise. As a result, our method facilitates efficient path planning based on reconstructed scene maps for UAV in GNSS-denied environment.

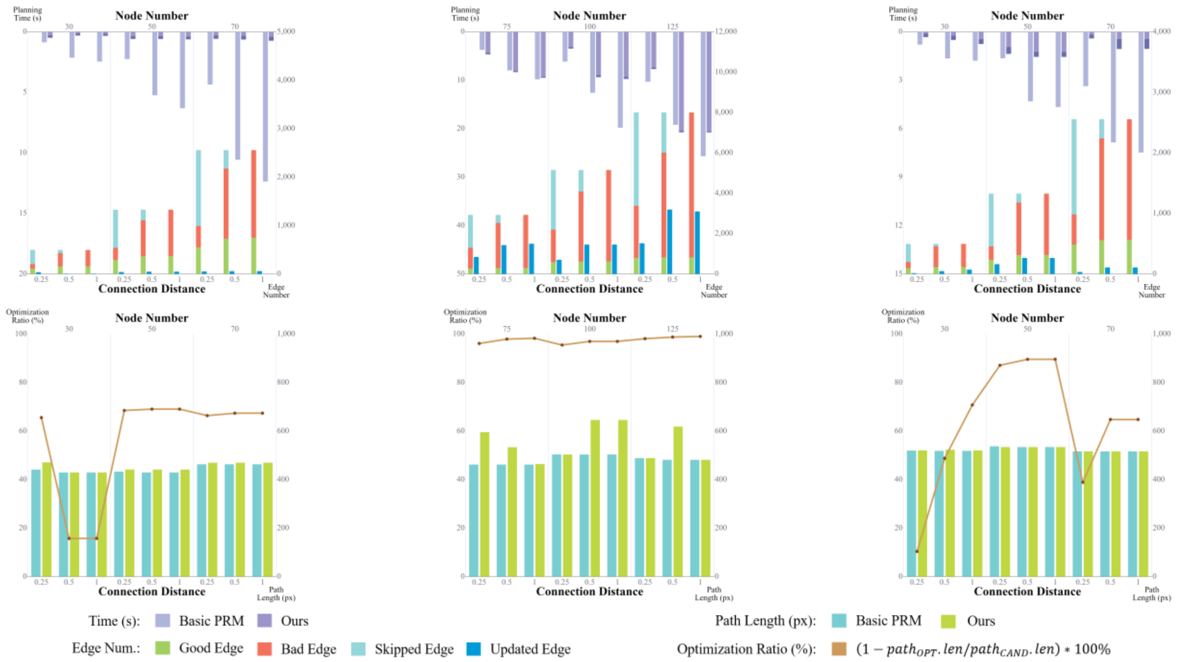

Figure 7. Visualization analysis of experimental results. The first row is the result of planning time, the second row is the result of path length. From left to right are Map 1, Map 2 and Map 3.

4. CONCLUSION AND DISCUSSION

In this paper, we proposed a method of 3D scene reconstruction and path planning for UAV in GNSS-denied environment. Our proposed path planning method greatly improves the computational efficiency compared to the basic PRM method, while our proposed path optimization method ensures reasonable path results. The UAV carrying LiDAR and IMU sensors, which can reconstruct the disaster site quickly and perform autonomous flight and navigation after path planning, provides a promising approach for disaster relief and rescue.

Focusing on reconstruction and planning in GNSS-denied environment, our method was originally designed for the scale of the indoor space of buildings and their outdoor surroundings after disasters. It is possible but not recommended that we use the method in large-scale situations, since there exists the localization drift problem caused by inadequate feature matching of SLAM, especially in open and spacious outdoor environment. Fortunately, however, it is not difficult to integrate GNSS into our method through data fusion techniques. In this way, SLAM is used for localization and modeling in key areas while GNSS is used for global positioning and correction. Thus combining their respective advantages, we can further apply our solutions to disaster situations of a much larger scale, e.g., earthquakes, wildfires, floods, landslides.

To develop a method for integration of SLAM and GNSS will be a major direction for our future work. Besides, we are also going to improve the robustness of our method in more complex scenes, conduct further research on environment perception and try to apply our method to autonomous exploration.

ACKNOWLEDGEMENTS

This work is supported by the National Natural Science Foundation of China (NSFC) (No. 42101441) and the Fundamental Research Funds for the Central Universities.

REFERENCES

Bailey, T., Durrant-Whyte, H., 2006. Simultaneous localization and mapping (SLAM): Part II. *IEEE robotics & automation magazine*, 13(3), 108-117.

Chen, J., Zhou, Y., Gong, J., Deng, Y., 2019. An improved probabilistic roadmap algorithm with potential field function for path planning of quadrotor. *2019 Chinese Control Conference (CCC)*, 3248-3253.

Chiang, K.W., Tsai, G.J., Li, Y.H., El-Sheimy, N., 2017. Development of LiDAR-based UAV system for environment reconstruction. *IEEE Geoscience and Remote Sensing Letters*, 14(10), 1790-1794.

Dehbi, Y., Klingbeil, L., Plümer, L., 2020. UAV mission planning for automatic exploration and semantic mapping. *Int. Arch. Photogramm. Remote Sens. Spatial Inf. Sci.*, XLIII-B1-2020, 521-526.

Faigl, J., Váňa, P., 2018. Surveillance planning with Bézier curves. *IEEE Robotics and Automation Letters*, 3(2), 750-757.

Ferguson, D., Stentz, A., 2007. Field D*: An interpolation-based path planner and replanner. *Robotics research*, 239-253.

Hart P.E., Nilsson N.J., Raphael B., 1968. A formal basis for the heuristic determination of minimum cost paths. *IEEE transactions on Systems Science and Cybernetics*, 4(2), 100-107.

Hofmann-Wellenhof, B., Lichtenegger, H., Wasle, E., 2007: *GNSS–global navigation satellite systems: GPS, GLONASS, Galileo, and more*. Springer Science & Business Media.

Indelman, V., Williams, S., Kaess, M., Dellaert, F., 2012. Factor graph based incremental smoothing in inertial navigation systems. *2012 15th International Conference on Information Fusion*, 2154-2161.

Kaku, K., 2019. Satellite remote sensing for disaster management support: A holistic and staged approach based on case studies in Sentinel Asia. *International Journal of Disaster Risk Reduction*, 33, 417-432.

Karam, S., Lehtola, V., Vosselman, G., 2020. Strategies to integrate IMU and LiDAR SLAM for indoor mapping. *ISPRS Ann. Photogramm. Remote Sens. Spatial Inf. Sci.*, V-1-2020, 223-230.

Kohlbrecher, S., Von Stryk, O., Meyer, J., Klingauf, U., 2011. A flexible and scalable SLAM system with full 3D motion estimation. *2011 IEEE international symposium on safety, security, and rescue robotics*, 155-160.

Rees, W.G., 2013: *Physical principles of remote sensing*. Cambridge university press.

Shan, T., Englot, B., Meyers, D., Wang, W., Ratti, C., Rus, D., 2020. LIO-SAM: Tightly-coupled LiDAR inertial odometry via smoothing and mapping. *2020 IEEE/RSJ international conference on intelligent robots and systems (IROS)*, 5135-5142.

Stoican, F., Prodan, I., Popescu, D., Ichim, L., 2017. Constrained trajectory generation for UAV systems using a b-spline parametrization. *2017 25th Mediterranean Conference on Control and Automation (MED)*, 613-618.

Welch, G.F., 2020. Kalman filter. *Computer Vision: A Reference Guide*, 1-3.

Xu, M., Wei, S., Zlatanova, S., Zhang, R., 2017. BIM-based indoor path planning considering obstacles. *ISPRS Ann. Photogramm. Remote Sens. Spatial Inf. Sci.*, IV-2/W4, 417-423.

Xu, W., Zhang, F., 2021. Fast-LIO: A fast, robust LiDAR-inertial odometry package by tightly-coupled iterated Kalman filter. *IEEE Robotics and Automation Letters*, 6(2), 3317-3324.

Yin, G.Y., Zhou, S.L., Wu, Q.P., 2017. An improved RRT algorithm for UAV path planning. *ACTA ELECTONICA SINICA*, 45(7), 1764.

Zhang, J., Singh, S., 2014. LOAM: LiDAR odometry and mapping in real-time. *Robotics: Science and Systems*, 2(9), 1-9.

Zhang, S., Liu, C., Haala, N., 2020. Three-dimensional path planning of UAVs imaging for complete photogrammetric reconstruction. *ISPRS Ann. Photogramm. Remote Sens. Spatial Inf. Sci.*, V-1-2020, 325-331.